

## Magnetostriction Assessment with Strain Gauges and Fiber Bragg Gratings

Cassiano C. Linhares<sup>1</sup>, João Espírito Santo<sup>1</sup>, Ricardo R. Teixeira<sup>1</sup>, Cristiano P. Coutinho<sup>1</sup>, Sérgio M.O. Tavares<sup>1</sup>, Marta Pinto<sup>1</sup>, João S. Costa<sup>1</sup>, Helder Mendes<sup>1</sup>, Catarina S. Monteiro<sup>2</sup>, António V. Rodrigues<sup>2</sup>, Orlando Frazão<sup>2</sup>

<sup>1</sup>Efacec, S. Mamede de Infesta, Porto, Portugal; <sup>2</sup>INESC TEC and Physics and Astronomy Department, Faculty of Sciences, University of Porto, Porto, Portugal

### Abstract

Power transformers have an imperative role in the future developments of the electrical grids. Treated as crucial assets for transportation and distribution of electrical energy, transformers are currently being studied regarding to the integration of technologies aiming to diagnose problems and monitoring data of electrical power grid. Furthermore, environmental noise pollution has gained importance, especially in active units of the power grid, located near consumers, such as transformers. Transformers noise can be classified according to its source: core, windings and cooling. This study addresses an experimental characterization of one of the main causes of transformers core noise - magnetostriction of electrical steel. An evaluation of magnetostriction properties of electrical steel, including resistive strain gauges and Fiber Bragg Gratings (FBGs) measurements with an Epstein frame, are presented and discussed. The magnetic flux density influence on hysteretic strain behavior of magnetostriction was evaluated, as well as the effect of a clamping load on core joints. Nowadays, optical interrogators for Bragg gratings have a high acquisition frequencies and wavelength sensitivity when compared to former optical interrogation systems, allowing to evaluate physical phenomena without electromagnetic interference and with equivalent resolution of conventional strain gauges.

Received on 12 April 2019; accepted on 30 October 2019; published on 13 November 2019

**Keywords:** Epstein Frame, FBGs, Magnetostriction, Noise, Power Transformers, Strain Gauges

Copyright © 2019 Cassiano C. Linhares *et al.*, licensed to EAI. This is an open access article distributed under the terms of the Creative Commons Attribution license (<http://creativecommons.org/licenses/by/3.0/>), which permits unlimited use, distribution and reproduction in any medium so long as the original work is properly cited.

doi:10.4108/eai.13-7-2018.161420

### 1. Introduction

The transformation of energy systems in smart energy networks represents a great challenge for power transformer manufacturers. In short term, developments in the field of smart grids will require a new generation of power transformers with the capability of monitoring, control and prevent surge problems – Digital Transformation - leading to the propagation of smart transformers.

The developing of future architectures of transformers is in this way strongly connected with power controllers and semiconductor devices – Solid State Transformers - fitting to operate in smart grids environments with fully automated electronic systems, which make it

a serious candidate for the replacement of traditional power transformers [1].

Nowadays, more importance is given to noise pollution, what has yielded several regulations and directives that specify the maximum noise levels in sensitive zones, such as urban areas [2].

In spite of being stationary machines, the active part of power transformers is a source of noise due to mechanical vibrations resulting from electromagnetic forces and magnetomechanical effects. Due to the increasing demands on power supply, more and more transformers are set near the final consumer, subjecting manufacturers to more restrictive specifications regarding noise levels.

Transformers noise can be classified according to its source: core noise, instigated by the magnetostriction of the transformer core and by the Maxwell forces; load noise, caused by the action of electromagnetic

\*Corresponding author. Email: [cassiano.linhares@efacec.com](mailto:cassiano.linhares@efacec.com)

†Corresponding author. Email: [joao.espiritosanto@efacec.com](mailto:joao.espiritosanto@efacec.com)

forces on the windings; cooling noise, which is due to auxiliary cooling equipment. According to several studies [3–5], core noise is the dominant source of noise for transformers whose rating is below 150 MVA. Since transformers rated power is usually lower near consumption, the mitigation of core noise has been the focus of many studies during the past years [6].

Due to the complexity of this phenomenon, an analytical model is not capable of accurately predict transformers noise level. Therefore empirical models [5] or numerical methods, are used to estimate the noise radiation of a power transformer. With the development of the numerical methods, as the finite element method (FEM) or the boundary element method (BEM), more accurate and detailed solutions are possible to be calculated. The development of such FEM/BEM models requires specific material properties that are not easily available, as the magnetomechanical behavior of the electrical steel. These properties need to be evaluated through representative sheet samples and representative experimental set-ups.

This paper presents an experimental set-up in which magnetostriction measurements were carried out, based on an Epstein frame. Strain data, directly related to magnetostriction measurements, is simultaneously collected using two distinct types of sensors: a resistive strain gauge, and an optical Fiber Bragg Grating (FBG). These measurements are the first step to compute the sound power level of a power transformer, providing inputs required by a commercial FEM software to predict magnetostriction along the transformer core, based on the magnetic field it is subjected to. The workflow of this numerical study is presented on Figure 1.

## 2. Background and Related Work

When magnetized, an electrical steel material is subjected to a mechanical deformation which varies with the magnetic polarization. This magnetomechanical effect, labeled magnetostriction, is one of the causes of transformers core vibration, along with the Maxwell forces (which occur when the magnetic field faces a material of different magnetic permeability). Magnetostriction is an anisotropic material property with non-linear behavior, which is specific of each type of electrical steel, and thus it may only be determined

experimentally.

The measurement of these properties can be performed with different set-ups, one of them is the Epstein frame. An Epstein frame comprises a primary and a secondary windings, disposed in four coils, and the testing specimens, forming an unloaded transformer, whose specifications are defined according to IEC standard 60404-2 [7]. This device may also be used to characterize the magnetomechanical behavior of the tested specimen, as described by the Technical Report IEC TR 62581 [8]. In this report, the general principles and technical details regarding magnetostriction measurements by means of an Epstein frame or a Single Sheet Tester are addressed.

The major part of the work developed on magnetostriction measurements was carried by means of a Single Sheet Tester, mainly because of its simplicity. Anderson et al. [9] developed a Single Sheet Tester which was capable to measure magnetostriction, under applied mechanical stress, using a piezoelectric accelerometer. Klimczyk et al. [10] improved the experimental set-up idealized by Anderson to study the influence of the specimen thickness, coating and residual stresses on the magnetostrictive behavior of electrical steel. Javorski et al. [11, 12] studied the frequency characteristics of magnetostriction using a modified Single Sheet Tester and formulated a numerical magnetostriction model based on those measurements. Ghalamestani [13] also used a Single Sheet Tester to carry out magnetostriction measurements, but instead of using accelerometers to measure the deformation, the author used an heterodyne laser interferometer.

However, an Epstein frame has better resemblance to the power transformer operation, since the effects of the lamination stacking, and clamping might not be neglected. Behlacen [14] studied magnetostriction by means of an Epstein frame, using a force transducer to compute the magnetostrictive forces and then converted them to deformation and strain values.

The application of sensors inside of electrical environments presents some challenges due to electromagnetic noise. Conventional electrical-based sensors can be affected by this electromagnetic interference. In addition, these sensing units are subjected to electrical discharges, which may damage this kind of sensors and

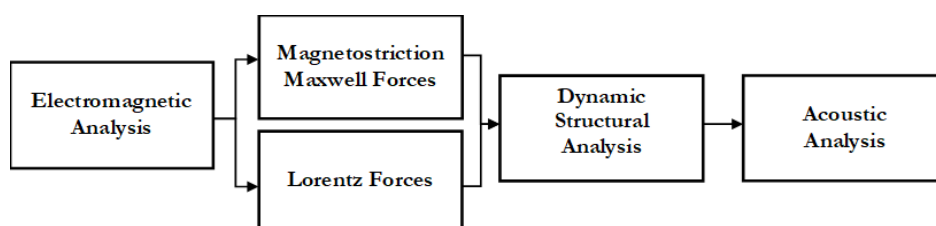


Figure 1. Numerical simulations workflow.

badly damage the instrumented structure. Fiber optic sensors offer the possibility to overcome these limitations due to its working principle – light. The optical fiber itself is immune to electromagnetic interference and it is made of high dielectric constant material [13, 15].

Nonetheless, the application of fiber optics inside large power transformers present other challenges. Optical fiber needs to be compatible with the oil inside the casing and needs to withstand high temperatures. The flexibility and resistance of fiber optics are among the main advantages comparing to other optical devices, but in order to grant the long term protection and to avoid accidental destruction of the sensor, the use of high temperature resistant polymers has been reported recently for different kinds of optical sensors [16, 17]. However, for tests with Epstein frame, where oil is not present, this technology is an optimal alternative compared with resistive strain gauges.

The present work aims to acquire and to evaluate the anisotropic magnetostriction and the influence of magnetic polarization and clamping loads applied on the joints of an electrical steel sheet, in order to update FEM models used to predict the radiated noise of power transformers. Additionally, using strain gauges and optical FBGs strain sensors, magnetostriction frequency characteristics were also studied.

### 3. Experimental Measurements

The magnetostriction measurements were carried out on an Epstein frame, by means of strain gauges and optical FBGs strain sensors. The strain data was acquired and then processed by a data acquisition system, which synchronized the strain signal with other obtained signals (current, voltage). The Epstein frame used in this work, Figure 2, matches the characteristics listed on the IEC standard previously referred [7].

Test specimens were assembled according to standard, in double lapped joints [7] and with their rolling direction parallel to the magnetizing direction [11].

**Electrical Steel Specimens.** In order to test electrical steel that is used in power transformers, several strips of grain oriented electrical steel *PowerCore*<sup>®</sup> H105-30 from ThyssenKrupp were collected. The characteristics of the tested electrical steel are shown in Table 1. Electrical strips dimensions were determined based on IEC/TR-62581, to ensure a magnetic path of 0.94 m [7].

**Strain Sensing.** For a punctual and local measurement of magnetostriction, both strain gauges and FBGs were used and placed in strips of the tested specimen. The chosen strain rosette has a temperature response matched to steel (HBM K-XY31-3/350) and two measuring grids (0°/90° T rosette).

The coating of the electrical strip was removed

allowing a direct strain measurement in the steel. The strain gauge was attached to the strip using an HBM Z70 adhesive, and connected to the data acquisition system with AWM 2651 cables. These cables were twisted, like shown on Figure 3, in an attempt to compensate electromagnetic interferences. In addition, to avoid the effects of the double-lap joints (test specimen edges) the gauge was positioned in the middle of the strip, like presented on Figure 3. The optical sensing set-up using the FBG was applied to the test strips in a similar configuration as the strain gauges, Figure 4. The FBGs were fabricated using the phase-mask method. This method starts by removing a section of the fiber coating, enabling the fiber to be directly exposed to the UV-light, through a phase-mask. The interference pattern of the UV-light engraves the desired grating with the modulation of the index of refraction along the fiber. After this process, the fiber is very fragile, thus it is recoated using polyimide. This recoating ensures protection of the FBG from mechanical and chemical hazards, also having a high temperature resistance. No special care was taken into account in relation to electromagnetic interference because the optical fiber is inert to it.

**Autotransformer.** In order to better control the voltage and current fed into the circuit, a Zenith V8HM autotransformer connecting the Epstein frame to the power supply, was used.

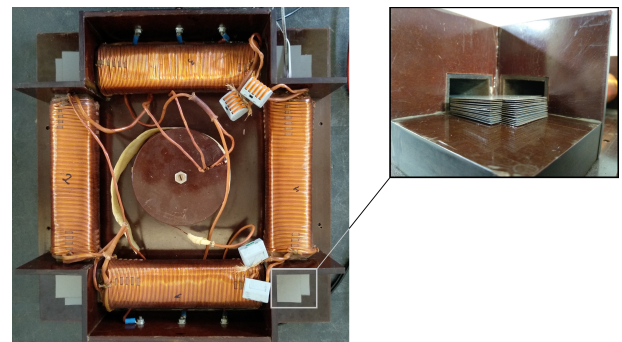


Figure 2. Epstein Frame.

Table 1. *PowerCore*<sup>®</sup> H105-30: material characteristics

Parameter	Value	Units
Saturation Polarization	2.03	T
Coercive Field Strength	5	A/m
Density	7650	kg/m <sup>3</sup>
Resistivity	0.48	μΩm
Length	300	mm
Width	30	mm
Thickness	0.3	mm

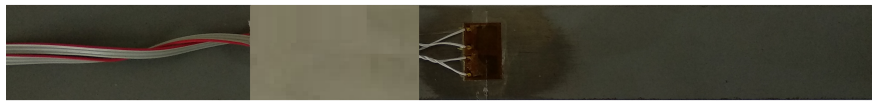


Figure 3. HBM strain gauge K-XY31-3/350 on the specimen.

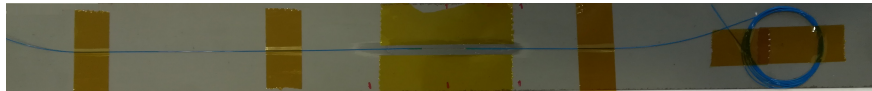


Figure 4. HBM FBG on the specimen.

**Data Acquisition System.** Data regarding current and voltage were acquired using NI-9227 and NI-9244 input modules, respectively, with a sampling time of 0.2 ms. This system allows the constant monitoring of magnetizing current and voltage supply in primary winding with a computer and a data logging software, NI Labview, as shown in Figure 5. For data acquisition from the resistive strain gauge, a National Instruments system composed by a CompactDAQ-9188 chassis and NI-9236 module were used, see Figure 6. The optical system was composed by a FBG strain sensor interrogated by a BraggScope FS26 (HBM FiberSensing) with a sampling time of 0.2 ms. Data from BraggScope was acquired using a BraggMonitor software as illustrated in Figure 7.

Through the data logging software, an interface algorithm was created, see Figure 8 to calculate magnetic field,  $H(t)$ , and magnetic polarization,  $B(t)$ , using Equations (1) and (2), where  $N_1$  and  $N_2$  are the number of turns of the primary and secondary windings, respectively,  $l$  the magnetic path length,  $I(t)$  is the current,  $A$  the magnetic active area and  $U_2(t)$  the voltage on the secondary winding [18, 19]. As a result, magnetostriction could be plotted as a function of  $B(t)$  or  $H(t)$ .

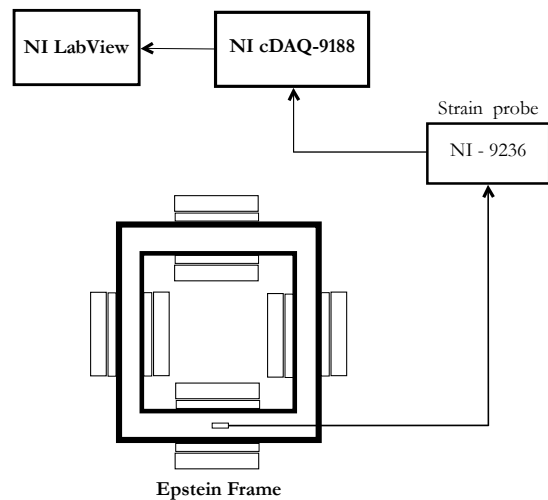


Figure 6. Strain gauge data acquisition - experimental set-up.

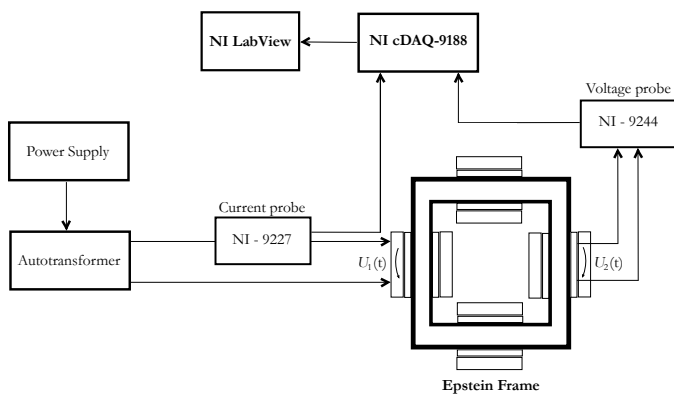


Figure 5. Electromagnetic excitation - experimental set-up.

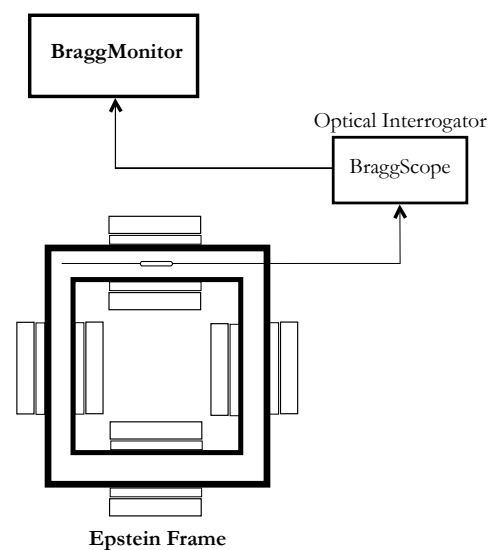


Figure 7. FBG data acquisition - experimental set-up.



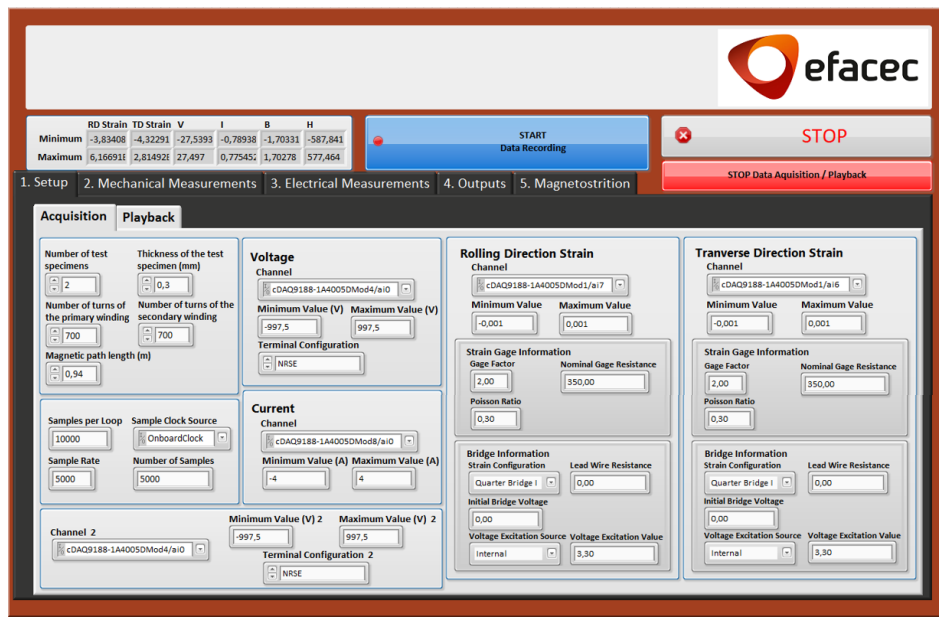


Figure 8. Screenshot of the graphical user interface.

$$H(t) = \frac{N_1 \cdot I(t)}{l} \quad (1)$$

$$B(t) = -\frac{1}{N_2 \cdot A} \int U_2(t) dt \quad (2)$$

### 3.1. Measurement Procedure

The excitation was made using the power grid ( $f \approx 50$  Hz and  $U_{rms} = 230$  V), by means of the auto-transformer, which allows the step-down and control of the voltage applied to the primary winding, Figure 9 .

Before starting the experimental data acquisition, preliminary calculations were performed for variables definition. Peak magnetic polarization ( $B_{peak}$ ) is predicted based on the effective secondary winding voltage ( $U_{2rms}$ ). Finally, the power supply output should be slowly increased until the secondary voltage has reached the desired value [7]. When the desired peak magnetic induction is achieved, the data is collected.

In a first stage, a combination of parameters such magnetic polarization (1.5, 1.7 and 1.9 T), number of laminations (1, 4 and 13 strips per limb) and clamping loads on the core joints (1.6 N) were studied using a strain gauge. A total of eighteen experimental measurements were done.

After analyzing these results, five experimental measurements using an FBG strain sensor were used for comparison with resistive strain gauge, considering six magnetic polarizations. A FFT (Fast Fourier Transform) were calculated for both strain sensors, for frequency range up to 500 Hz.

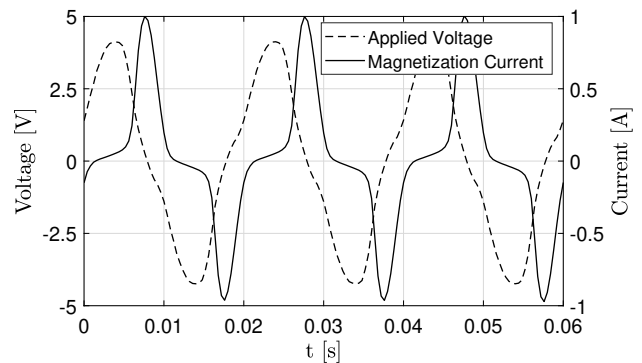
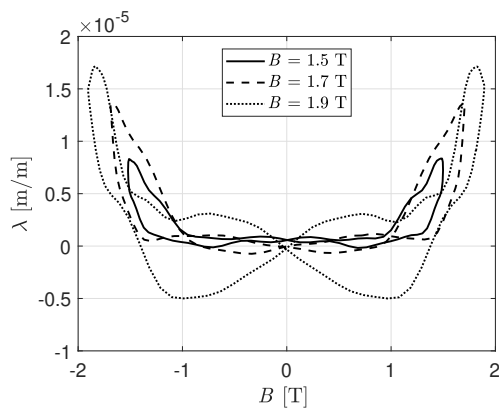


Figure 9. Voltage applied to the primary winding and magnetization current (1 strip per limb).

## 4. Results and Discussion

Initially, magnetostriction frequency characteristics were studied. According to literature review [11], for an excitation frequency of 50 Hz, magnetostriction presents a fundamental component of 100 Hz (double the excitation frequency), and respective harmonics (multiples of the fundamental component). However, the acquired signal exhibited a distorted behavior, possibly due to electromagnetic interference, especially when compared to those of IEC TR-62581 [8].

Therefore, to ensure a representative magnetostriction loop, a FFT analysis was conducted. Through this analysis, it was concluded that, in addition to the fundamental component, other harmonics were present, some of which were related with magnetostriction multiple harmonics, the others were related with the power



**Figure 10.** Magnetostriction as a function of the magnetic polarization using strain gauges (13 strips per limb).

grid (50 Hz and uneven harmonics) and other parasite signals.

The influence of the magnetic polarization on the magnetostriction of the test specimen was also addressed. According to previous studies [9, 13], peak-to-peak magnetostriction rises when the magnetic polarization increases. This trend was verified in the tested specimen, as shown in Figure 10. Moreover, the magnetostriction loop is distorted when polarization rises, especially when the polarization is beyond the knee point of the hysteresis loop (B-H). This fact may be explained by a greater influence of higher harmonics (300 Hz and higher) on the magnetostrictive behavior of the specimen, as can be seen in Figure 11.

The impact of a clamping load on the lap joints of the Epstein frame, as displayed in Figure 12, was also investigated. In order to load the joints, four 1.6 N weights were used. Figures 13 and 14 show the measured results. It was verified that the magnetostriction loops were distorted, yet the peak-to-peak and zero-to-peak magnetostriction values remained the same. The curve of higher polarization was the most misshaped, to the extent that the compressive strain could no longer be observed.

To work around the problem, magnetostriction fundamental frequency and respective harmonics were identified and isolated. Figure 11 shows the magnetostriction spectrum for an iron core composed by thirteen steel sheets per limb, under three induction levels. As it can be verified, the first two harmonics (100 and 200 Hz) show a greater contribution; however, for higher polarization values, the influence of higher harmonics rises.

As said before, a comparison between FBGs strain sensor and resistive strain gauge was made and the average results of magnitude are shown in Figure 15 to Figure 20. Looking for more relevant frequencies, 100 and 200 Hz, the results show that the FBG sensor present

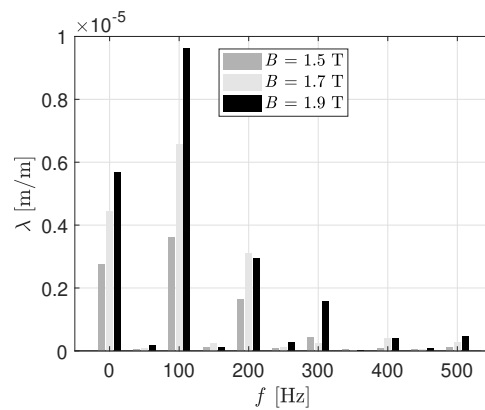


**Figure 11.** Magnetostriction frequency spectrum using strain gauges.

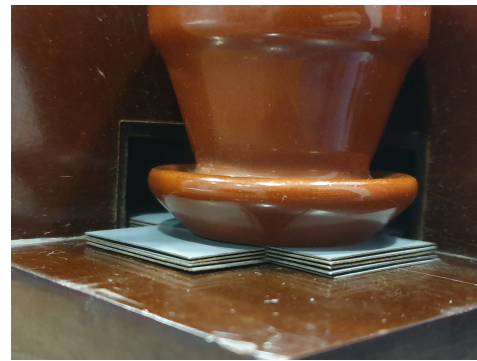


**Figure 12.** Load applied on the lap joints.

always the lowest values of peak-to-peak amplitude. This could be explained by the electromagnetic noise on the resistive strain gauge. Also, a more constant and lower values between the five tests were obtained on the optical FBG strain sensor compared with resistive strain gauge. This variability shows again that the resistive strain gauge signal is more sensitive to external noise. Comparing the amplitude of magnetic polarization for 100 Hz, an approximated linear relation between magnetostriction and magnetic polarization is verified.

Besides, this study revealed that the applied load on the core joints has influence on the hysteretic behavior of magnetostriction, since the oscillation in the normal component was constrained. Having low amplitude, magnetostriction is sensitive to other effects.

Regarding the obtained results, the magnetostriction loop can be applied to numerical simulations, allowing the evaluation of power transformer noise radiation.

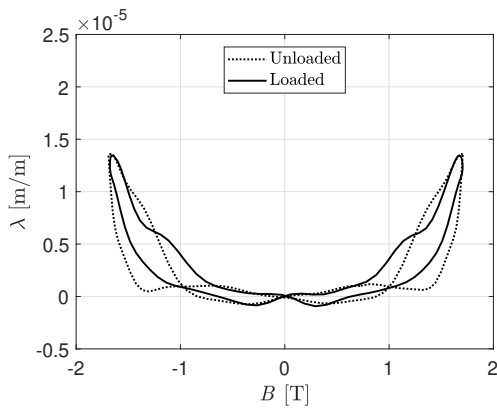


**Figure 13.** Influence of a clamping load applied on the core joints for a peak magnetic polarization of 1.7 T.

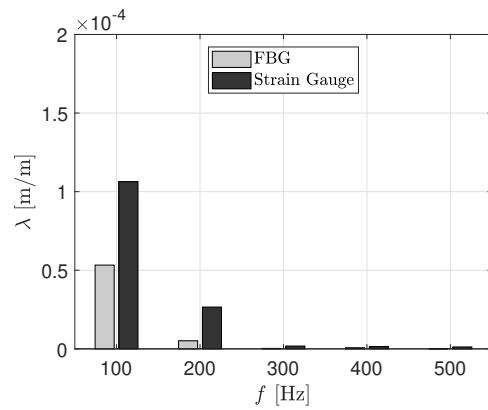


**Figure 16.** Magnetostriction for a peak magnetic polarization of 1.5 T (1 strip per limb).

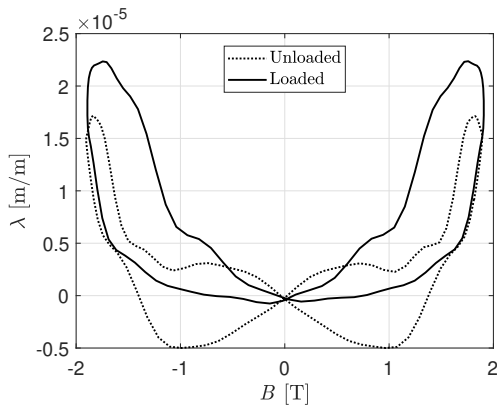


**Figure 14.** Influence of a clamping load applied on the core joints for a peak magnetic polarization of 1.9 T.

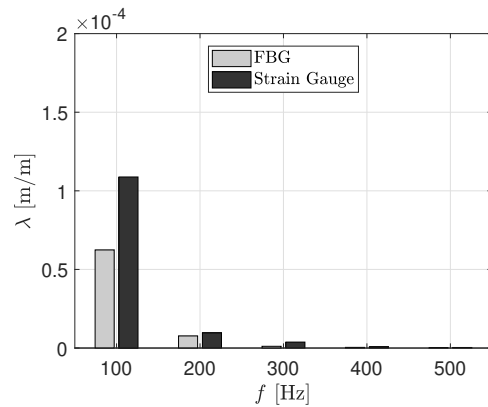


**Figure 17.** Magnetostriction for a peak magnetic polarization of 1.7 T (1 strip per limb).

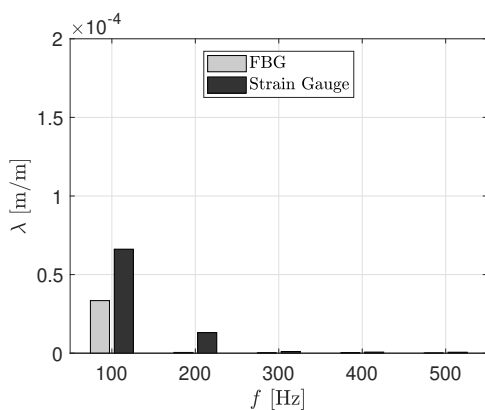


**Figure 15.** Magnetostriction for a peak magnetic polarization of 1.3 T (1 strip per limb).

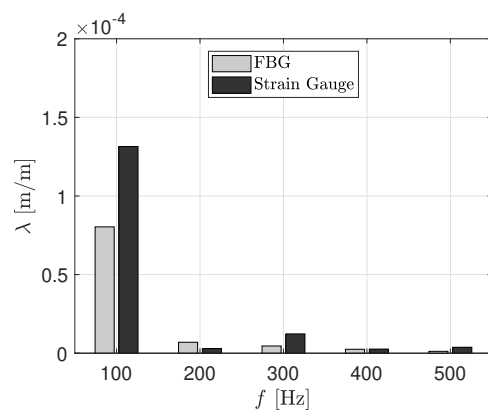


**Figure 18.** Magnetostriction for a peak magnetic polarization of 1.9 T (1 strip per limb).

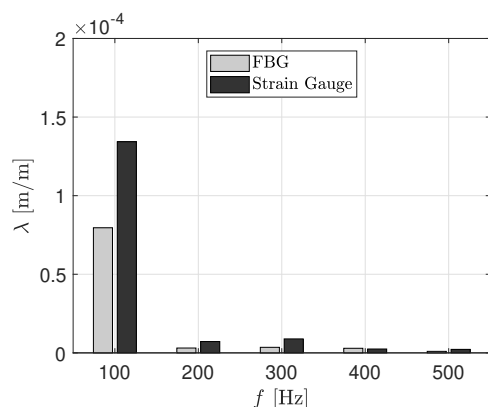


**Figure 19.** Magnetostriction for a peak magnetic polarization of 2.0 T (1 strip per limb).

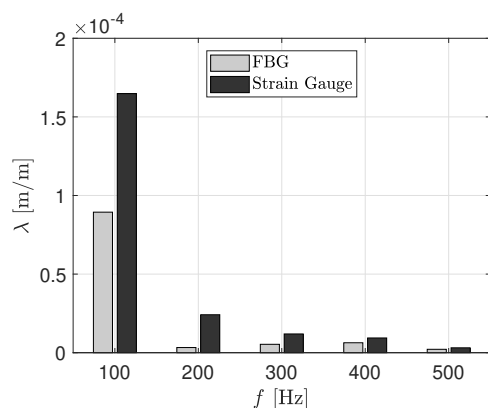


**Figure 20.** Magnetostriction for a peak magnetic polarization of 2.1 T (1 strip per limb).

## 5. Conclusions

Magnetostrictive behavior of grain oriented electrical steel was studied by means of an experimental set-up based on an Epstein frame. For the magnetostriction measurements, the generated signal of a strain gauge rosette and FBG strain sensor was acquired and then processed via data logging software. Current and voltage data was also acquired and synchronized with the strain data, so that the magnetostriction curves could be obtained.

The frequency characteristics of magnetostriction were also addressed. The obtained results allowed to conclude that the first two harmonics are the most significant, yet when the magnetic flux density gets closer to saturation, higher harmonics gain more influence.

Measurements with fiber Bragg gratings showed lower magnetostriction values when compared with the resistive strain gauges. The influence of the electromagnetic field of the Epstein frame windings can be noteworthy, compromising the measured materials properties. This study demonstrates that

the application of optical sensing technologies, as the FBGs, give a more reliable material data about the magnetostriction behaviour, required for numerical studies.

## Acknowledgements

This work is a result of the project POCI-01-0247-FEDER-024035, with the designation “Quiet Transformer 2”, supported by Competitiveness and Internationalisation Operational Programme (POCI), under the PORTUGAL 2020 Partnership Agreement, through the European Regional Development Fund (ERDF).

C.S. Monteiro was funded by FCT - Portuguese national funding agency for science, research and technology (SFRH/BD/135820/2018).

## References

- [1] A Abu-Siada, Jad Budiri, and Ahmed Abdou. Solid state transformers topologies, controllers, and applications: State-of-the-art literature review. *Electronics*, 7:298, 11 2018. doi:10.3390/electronics7110298.
- [2] *Special Eurobarometer 468: “Attitudes of European citizens towards the environment”*. European Commission, November 2017.
- [3] Luis Fernández Braña, Hugo M.R. Campelo, and Xosé M. López-Fernández. Quiet transformers: Design issues. *Advanced Research Workshop on Transformers (ARWtr)*, 2013.
- [4] S. L. Foster and E. Reiplinger. Characteristics and Control of Transformer Sound. *IEEE Transactions on Power Apparatus and Systems*, PAS-100(3):1072–1077, 1981.
- [5] Ramsis S Girgis, Mats Bernesjo, and Jan Anger. Comprehensive analysis of load noise of power transformers. In *Power & Energy Society General Meeting, 2009. PES'09. IEEE*, pages 1–7. IEEE, 2009.
- [6] C.P. Coutinho; C. Novais; S.M.O. Tavares; M. Pinto; A. Vieira; C.C. Linhares; H. Mendes; R. Castro Lopes. Dynamic response of power transformer tanks. Proceedings of the IEEE 2018 9th Power, Instrumentation and Measurement Meeting (EPIM), November 2018.
- [7] IEC/60404-2. Methods of measurement of the magnetic properties of electrical steel strip and sheet by means of an Epstein frame, June 2008.
- [8] IEC/TR-62581. Electrical steel-Methods of measurements of the magnetostriction characteristics by means of single sheet and Epstein test specimens. Technical report, International Electrotechnical Commission, 2010.
- [9] P.I. Anderson, A.J. Moses, and HJ Stanbury. An automated system for the measurement of magnetostriction in electrical steel sheet under applied stress. *Journal of magnetism and magnetic materials*, 215:714–716, 2000.
- [10] Piotr Klimczyk. *Novel techniques for characterisation and control of magnetostriction in GOSS*. PhD thesis, Cardiff University, 2012.



- [11] Matija Javorski, Janko Slavič, and Miha Boltežar. Frequency characteristics of magnetostriction in electrical steel related to the structural vibrations. In *IEEE Transactions on Magnetism*, volume 48, pages 4727–4734. IEEE, 2012.
- [12] Matija Javorski, Gregor Čepon, Janko Slavič, and Miha Boltežar. A generalized magnetostrictive-forces approach to the computation of the magnetostriction-induced vibration of laminated steel structures. In *IEEE Transactions on Magnetism*, volume 49, pages 5446–5453. IEEE, 2013.
- [13] Setareh Gorji Ghalamestani. *Magnetostriction in electrical steel: numerical modelling and development of an optical measurement method*. PhD thesis, Ghent University, 2013.
- [14] Anouar Belahcen. *Magnetoelasticity, Magnetic Forces and Magnetostriction in Electrical Machines*. PhD thesis, Helsinki University of Technology, 2004.
- [15] Anees Mohammed and Siniša Djurović. A study of distributed embedded thermal monitoring in electric coils based on FBG sensor multiplexing. *Microprocessors and Microsystems*, 62:102–109, 2018.
- [16] Peter Kung, Robert Idsinga, H-Chaska V Durand, Hua Lu, and Mojtaba Kahrizi. Fiber optics sensor monitoring moisture transport in oil in an operating transformer. In *2017 IEEE Electrical Insulation Conference (EIC)*, pages 487–490. IEEE, 2017.
- [17] Guo-Ming Ma, Hong-Yang Zhou, Cheng Shi, Ya-Bo Li, Qiang Zhang, Cheng-Rong Li, and Qing Zheng. Distributed partial discharge detection in a power transformer based on phase-shifted FBG. *IEEE Sensors Journal*, 18(7):2788–2795, 2018.
- [18] Satish V Kulkarni and SA Khaparde. *Transformer engineering: design, technology, and diagnostics*. CRC Press, 2013.
- [19] Péter Kis, Miklós Kuczmann, János Füzi, and Amália Iványi. Hysteresis measurement in Labview. *Physica. B*, 343:357–363, 2004.